

Supporting Information

Nucleus-localized Platinum(II)-Triphenylamine Complexes as Potent Photodynamic Anticancer Agents

*Yi-Fang Zhong,[‡] Hang Zhang,[‡] Ge Mu, Wen-Ting Liu, Qian Cao, Cai-Ping Tan, Liang-Nian Ji, and Zong-
Wan Mao**

MOE Key Laboratory of Bioinorganic and Synthetic Chemistry, School of Chemistry, Sun Yat-Sen
University, Guangzhou, 510275

E-mail: cesmzw@mail.sysu.edu.cn

Table of Contents

Experimental Section	S4
Figure S1 ¹ H-NMR spectrum of 1	S13
Figure S2 ¹³ C-NMR spectrum of 1	S13
Figure S3 ¹⁹⁵ Pt-NMR spectrum of 1	S14
Figure S4 ESI-MS spectrum of 1	S14
Figure S5 ¹ H-NMR spectrum of 2	S15
Figure S6 ¹³ C-NMR spectrum of 2	S15
Figure S7 ¹⁹⁵ Pt-NMR spectrum of 2	S16
Figure S8 ESI-MS spectrum of 2	S16
Figure S9 ¹ H-NMR spectrum of 3	S17
Figure S10 ¹³ C-NMR spectrum of 3	S17
Figure S11 ¹⁹⁵ Pt-NMR spectrum of 3	S18
Figure S12 ESI-MS spectrum of 3	S18
Figure S13 ¹ H-NMR spectrum of 4	S19
Figure S14 ¹³ C-NMR spectrum of 4	S19
Figure S15 ¹⁹⁵ Pt-NMR spectrum of 4	S20
Figure S16 ESI-MS spectrum of 4	S20
Figure S17 Time dependent UV-Vis spectra of 1-4 in PBS.....	S21
Figure S18 Time dependent ¹ H-NMR spectra of 1-4 in <i>d</i> ₆ -DMSO/H ₂ O.....	S22
Figure S19 ESR signal of radicals induced by 1-4 and trapped by TEMP..	S23

Figure S20	$^1\text{O}_2$ quantum yield of 1-4 measured upon 365 nm irradiation.....	S24
Figure S21	UV-Vis titration with ssDNA and K_b calculation.....	S25
Figure S22	UV-Vis titration with ds26 and K_b calculation.....	S26
Figure S23	UV-Vis titration with 22AG and K_b calculation.....	S27
Figure S24	Fluorescence titration with ssDNA.....	S28
Figure S25	Fluorescence titration with ds26.....	S29
Figure S26	Fluorescence titration with 22AG.....	S30
Figure S27	Colocalization studies of 1-4	S31
Figure S28	Confocal microscopy images of L1 •3HCl and L2 •3HCl.....	S32
Figure S29	Effects of 1-4 on cellular ROS production in dark condition.....	S33
Figure S30	Effects of NAC on the viability of HeLa cells upon PDT treatments....	S34
Figure S31	Effects of L1 and L2 on cellular ROS production.....	S35
Figure S32	Quantitative cell-cycle distribution data of 2	S36
Figure S33	Body weight change of tumor-bearing mice with different treatments..	S37
Figure S34	H&E staining of the major organs after different treatments.....	S38
Table S1	Summary of DNA binding constants of 1-4	S39
References		S39

Experimental Section

Materials and Methods. Cisplatin (Sigma Aldrich, USA), transplatin (Alfa Aesar, USA), tris(4-bromophenyl)amine (J&K Scientific Ltd., China), pyridine-4-boronic acid (J&K Scientific Ltd., China), pyridine-3-boronic acid (J&K Scientific Ltd., China), Pd(PPh₃)₄ (Sigma Aldrich, USA), DMSO (Sigma Aldrich, USA), MTT (3-(4,5-dimethylthiazol-2-yl)-2,5-diphenyltetrazolium bromide, Sigma Aldrich, USA), ABDA (Sigma Aldrich, USA), [Ru(bpy)₃]Cl₂ (Sigma Aldrich, USA), SYTO-82 (Life Technologies, USA), LTDR (Life Technologies, USA), MTDR (Life Technologies, USA), PI (Sigma Aldrich, USA), PBS (phosphate buffered saline, Sigma Aldrich, USA), NAC (Sigma Aldrich, USA), DCFH-DA (Sigma Aldrich, USA) and pBR322 plasmid DNA (Life Technologies, USA) were used as received.

¹H-NMR, ¹³C-NMR and ¹⁹⁵Pt-NMR spectra were recorded on a Bruker Advance 400 spectrometer (Germany). Elemental analysis (C, H, N) was carried out using an Elemental Vario EL CHNS analyzer (Germany). ESI-MS was measured with LCMS-2010 spectrometer (Japan). UV-Vis spectra were recorded on a Varian Carry 100 spectrophotometer (USA). Fluorescence emission spectra and lifetime measurements were performed on an Edinburgh FLS 920 spectrometer (UK). Fluorescence quantum yields at room temperature were calculated according to literature procedures using [Ru(bpy)₃](PF₆)₂ as the reference.¹

Synthesis and Characterization. The bridging ligand **L1** and **L2** were synthesized according to literature methods.²

Synthesis of {[cis-PtCl(NH₃)₂]₃L1}(NO₃)₃ (1**).** Cisplatin (90 mg, 0.30 mmol) and AgNO₃ (50.9 mg, 0.30 mmol) in DMF (6 mL) were stirred under an inert atmosphere of N₂ in darkness for 24 h at 40 °C and then centrifuged to remove AgCl. The clear liquid was subsequently transferred to another round bottom flask and then **L1** (42.9 mg, 0.09 mmol) was added. The mixture was heated at 85 °C for 48 h under N₂ in darkness. The final product was precipitated through the addition of diethyl ether and then collected by centrifugation, washed with methanol, dichloromethane and diethyl

ether and further dried in vacuum to obtain a yellow powder. Yield: 97.6 mg (74.4%). $^1\text{H-NMR}$ (400 MHz, d_6 -DMSO): δ = 8.72 (d, J = 6.7 Hz, 6H), 7.93 (dd, J = 19.1, 7.8 Hz, 12H), 7.28 (d, J = 8.7 Hz, 6H), 4.68 (s, 9H), 4.31 (s, 9H). $^{13}\text{C-NMR}$ (101 MHz, d_6 -DMSO): δ = 164.16, 154.70, 152.10, 150.15, 131.95, 130.58, 126.50, 124.31, 122.63 ppm; $^{195}\text{Pt-NMR}$ (86 MHz, d_6 -DMSO): δ = -2268.33 ppm with K_2PtCl_4 as the internal reference (δ = 0). ESI-MS (H_2O): m/z = 416.80 $[\text{M-3NO}_3\text{-Cl+H}_2\text{O-H}]^{3+}$, 422.90 $[\text{M-3NO}_3]^{3+}$, 502.45 $[\text{M-3NO}_3\text{-PtCl(NH}_3)_2]^{2+}$, 624.75 $[\text{M-3NO}_3\text{-Cl+H}_2\text{O-2H}]^{2+}$. Elemental analysis calcd (%) for $\{[\text{cis-PtCl(NH}_3)_2]_3\text{L1}\}(\text{NO}_3)_3$ (1456.38 g/mol): C, 27.21; H, 2.91; N, 12.50; found (%): C, 27.01; H, 3.06; N, 12.26.

Synthesis of $\{[\text{trans-PtCl(NH}_3)_2]_3\text{L1}\}(\text{NO}_3)_3$ (2). Transplatin (90 mg, 0.30 mmol) and AgNO_3 (50.9 mg, 0.30 mmol) in DMF (6 mL) were stirred under an inert atmosphere of N_2 in darkness for 24 h at 35 °C and then centrifuged to remove AgCl . The clear liquid was subsequently transferred to another round bottom flask and then **L1** (42.9 mg, 0.09 mmol) was added. The mixture was heated at 60 °C for 48 h under N_2 in darkness. The final product was precipitated through the addition of diethyl ether and then collected by centrifugation, washed with methanol, dichloromethane, and diethyl ether and further dried in vacuum to obtain a yellow powder. Yield: 94.5 mg (72.1%). $^1\text{H-NMR}$ (400 MHz, d_6 -DMSO): δ = 8.75 (d, J = 6.7 Hz, 6H), 8.08–7.89 (m, 12H), 7.28 (t, J = 7.9 Hz, 6H), 4.75 (s, 2H), 4.24 (s, 16H); $^{13}\text{C-NMR}$ (151 MHz, d_6 -DMSO): δ = 153.18, 150.19, 148.07, 129.85, 128.59, 124.57, 122.77 ppm; $^{195}\text{Pt-NMR}$ (86 MHz, d_6 -DMSO): δ = -2274.96 ppm with K_2PtCl_4 as the internal reference (δ = 0). ESI-MS (H_2O): m/z = 423.15 $[\text{M-3NO}_3]^{3+}$, 503.30 $[\text{M-3NO}_3\text{-PtCl(NH}_3)_2]^{2+}$, 635.30 $[\text{M-3NO}_3\text{-H}]^{2+}$, 657.45 $[\text{M-3NO}_3\text{+2Na-3H}]^{2+}$, 665.55 $[\text{M-3NO}_3\text{+2Na+H}_2\text{O-3H}]^{2+}$. Elemental analysis calcd (%) for $\{[\text{trans-PtCl(NH}_3)_2]_3\text{L1}\}(\text{NO}_3)_3$ (1456.38 g/mol): C, 27.21; H, 2.91; N, 12.50; found (%): C, 27.15; H, 3.02; N, 12.38.

Synthesis of $\{[\text{cis-PtCl(NH}_3)_2]_3\text{L2}\}(\text{NO}_3)_3$ (3). Cisplatin (90 mg, 0.30 mmol) and AgNO_3 (50.9 mg, 0.30 mmol) in DMF (6 mL) were stirred under an inert atmosphere of N_2 in darkness for 24 h at 40 °C and then centrifuged to remove AgCl . The clear liquid was subsequently transferred to another round bottom flask and then **L2** (42.9

mg, 0.09 mmol) was added. The mixture was heated at 85 °C for 48 h under N₂ in darkness. The final product was precipitated through the addition of diethyl ether and then collected by centrifugation, washed with methanol, dichloromethane and diethyl ether and further dried in vacuum to obtain a pale yellow powder. Yield: 95.8 mg (73.1%). ¹H-NMR (400 MHz, *d*₆-DMSO): δ = 9.00 (s, 3H), 8.71 (d, J = 5.5 Hz, 3H), 8.34 (d, J = 8.1 Hz, 3H), 7.81 (d, J = 8.6 Hz, 6H), 7.66 (dd, J = 7.9, 5.9 Hz, 3H), 7.28 (d, J = 8.5 Hz, 6H), 4.73 (s, 8H), 4.52 (s, 3H), 4.34 (s, 7H); ¹³C-NMR (101 MHz, DMSO): δ = 153.16, 152.02, 149.12, 139.08, 138.20, 135.55, 131.61, 130.39, 128.04, 126.45 ppm; ¹⁹⁵Pt-NMR (86 MHz, *d*₆-DMSO): δ = -2266.31 ppm with K₂PtCl₄ as the internal reference (δ = 0). ESI-MS (H₂O): m/z = 416.35 [M-3NO₃-Cl+H₂O-H]³⁺, 423.40 [M-3NO₃]³⁺, 635.00 [M-3NO₃-H]²⁺, 656.75 [M-3NO₃+2Na-3H]²⁺. Elemental analysis calcd (%) for {[cis-PtCl(NH₃)₂]₃L2}(NO₃)₃ (1456.38 g/mol): C, 27.21; H, 2.91; N, 12.50; found (%): C, 27.08; H, 3.16; N, 12.35.

Synthesis of {[trans-PtCl(NH₃)₂]₃L2}(NO₃)₃ (4). Transplatin (90 mg, 0.30 mmol) and AgNO₃ (50.9 mg, 0.30 mmol) in DMF (6 mL) were stirred under an inert atmosphere of N₂ in darkness for 24 h at 35 °C and then centrifuged to remove AgCl. The clear liquid was subsequently transferred to another round bottom flask and then L2 (42.9 mg, 0.09 mmol) was added. The mixture was heated at 80 °C for 48 h under N₂ in darkness. The final product was precipitated through the addition of diethyl ether and then collected by centrifugation, washed with methanol, dichloromethane and diethyl ether and further dried in vacuum to obtain a pale yellow powder. Yield: 91.7 mg (70.0%). ¹H-NMR (400 MHz, *d*₆-DMSO): δ = 9.08 (s, 3H), 8.73 (d, J = 5.4 Hz, 3H), 8.35 (d, J = 8.1 Hz, 3H), 7.84 (d, J = 8.7 Hz, 6H), 7.70–7.63 (m, 3H), 7.28 (t, J = 6.9 Hz, 6H), 4.79 (s, 3H), 4.26 (s, 15H); ¹³C-NMR (151 MHz, *d*₆-DMSO): δ = 162.20, 151.48, 150.92, 147.15, 137.47, 136.15, 129.71, 128.45, 126.59, 124.50 ppm; ¹⁹⁵Pt-NMR (86 MHz, *d*₆-DMSO): δ = -2273.87 ppm with K₂PtCl₄ as the internal reference (δ = 0). ESI-MS (H₂O): 423.25 [M-3NO₃]³⁺, 502.80 [M-3NO₃-PtCl(NH₃)₂]²⁺, 633.65 [M-3NO₃-H]²⁺, 656.55 [M-3NO₃+2Na-3H]²⁺, 666.90 [M-3NO₃+2Na+H₂O-3H]²⁺. Elemental analysis calcd (%) for {[trans-

PtCl(NH₃)₂]₃L2}(NO₃)₃ (1456.38 g/mol): C, 27.21; H, 2.91; N, 12.50; found (%): C, 27.32; H, 3.11; N, 12.31.

Electron Spin Resonance (ESR) Assay. The ESR measurements were carried out in a literature reported method³ with a Bruker Model A300 spectrometer at 298 K. The samples containing 10 μM of **1–4** in 10 mM Tris-HCl, pH = 7.4 buffer were loaded in glass capillary tubes and the spectra were recorded after irradiation (425 nm, 40 mW cm⁻², 10 min). All ESR measurements were carried out using the following settings: 20 mW microwave power, 100 G scan range, and 1 G field modulation. 2,2,6,6-tetramethylpiperidine (TEMP, J&K, 20 mM) was used for trapping ¹O₂.

¹O₂ Production Quantum Yields. The quantum yields for ¹O₂ production of the compounds under irradiation in aerated 10 mM Tris-HCl buffer solution (pH = 7.4) were evaluated according to a literature procedure.⁴ ABDA was used as the ¹O₂ indicator⁵ and [Ru(bpy)₃]Cl₂ as the standard ($\Phi_{\Delta} = 0.18$ in H₂O)⁶. Briefly, air-equilibrated buffer solutions containing the compounds and ABDA (100 μM) were prepared in the dark and irradiated with a 425 nm LED light. The absorption maxima of ABDA (380 nm at pH 7.4 buffer) were recorded every 5 s. The absorbance at 425 nm of the tested compounds and [Ru(bpy)₃]Cl₂ was kept at 0.15. The Φ_{Δ} of the compounds was calculated according to the following equation.

$$\Phi_{\Delta(x)} = \Phi_{\Delta(std)} \times \left(\frac{S_x}{S_{std}}\right) \times \left(\frac{F_{std}}{F_x}\right)$$

where subscripts x and std designate the sample and [Ru(bpy)₃]Cl₂, respectively. S stands for the slope of plot of the 380 nm wavelength absorption of ABDA against the irradiation time (s). F stands for the absorption correction factor, which is given by $F = 1 - 10^{-OD}$ (OD represents the optical density of sample and [Ru(bpy)₃]Cl₂ at 425 nm).

UV-Vis Absorption and Fluorescence Emission Titration Experiments. The oligonucleotide sequences used in these experiments were:

ssDNA: 5'-GGCATAGTGCGTGGGCG-3';

ds26: 5'-CAATCGGATCGAATTCGATCCGATTG-3';

22AG: 5'-AGGGTTAGGGTTAGGGTTAGGG-3'.

They were PAGE purified and purchased from Invitrogen (Shanghai, China). Before titration, complexes 1-4 (5 μ M) were dissolved in the corresponding buffer for 24 h to reach equilibrium. The intrinsic binding constant K_b of complexes 1-4 was obtained by fitting the data to the following equation described by Brad et.al.⁷ from a plot of $(\epsilon_a - \epsilon_f)/(\epsilon_b - \epsilon_f)$ vs. [DNA].

$$(\epsilon_a - \epsilon_f)/(\epsilon_b - \epsilon_f) = (b - (b^2 - 2K^2C[\text{DNA}]/s))^{1/2}/2KbC$$

$$b = 1 + KC + K[\text{DNA}]/2s$$

where C is the total complex concentration, [DNA] is the DNA concentration, and s is the binding site size. ϵ_a , ϵ_b , ϵ_f is the apparent extinction coefficient, the extinction coefficient of bound complex and the extinction coefficient of free complex.

Electrophoretic Mobility Shift Assay. Supercoiled pBR322 plasmid DNA (0.5 μ g/10 μ L) was incubated with increasing concentration of complex 1-4 (1 μ M-5 μ M) in 10 mM Tris-HCl, pH = 7.4 buffer at 37 $^{\circ}$ C for 30 min in the dark. Then the solutions were irradiated with 425 nm LED light (40 mW cm^{-2} , 10 min) or remained in the dark, after which the samples were incubated at 37 $^{\circ}$ C for another 2 h in the dark. The reactions were then quenched by adding 2 μ L of 6 \times loading buffer (Takara, Japan). The resulting mixtures were loaded onto a 0.9% agarose gel containing ethidium bromide (EB). Following the electrophoresis at 50 mV for 1.5 h in TBE buffer, the bands were visualized and photographed using UVP BioImaging Systems.

Cell culture. HeLa, HepG2, A549, A549cisR and LO2 were obtained from Experimental Animal Center of Sun Yat-Sen University (Guangzhou, China). Cells were maintained in DMEM (Dulbecco's modified Eagle's medium, Gibco BRL) or RPMI 1640 (Roswell Park Memorial Institute 1640, Gibco BRL) medium, supplemented with 10% FBS (fetal bovine serum, Gibco BRL), 100 μ g/mL streptomycin and 100 U/mL penicillin (Gibco BRL). Cells were cultured in a humidified 37 $^{\circ}$ C, 5% CO_2 /95% air (v/v) environment. In each experiment, cells treated with vehicle control (1% DMSO) were kept as the reference group.

Intracellular Localization Assay. For live cell imaging, HeLa cells were incubated with **1–4** (2 μ M) at 37 °C for 12 h and then washed three times with ice-cold PBS and visualized by confocal microscopy (LSM 710, Carl Zeiss, Göttingen, Germany) with a 63 \times oil-immersion objective lens immediately. The wavelengths for excitation of **1–4** were 405 nm. Emission was collected at 480–580 nm.

For colocalization assay, HeLa cells were incubated with **1–4** (2 μ M) at 37 °C for 6 h and further co-incubated with SYTO-82 (1 μ M), LTDR (150 nM) or MTDR (150 nM) at 37 °C for another 0.5 h. Cells were washed three times with PBS and visualized by confocal microscopy. The excitation wavelength of SYTO-82, LTDR and MTDR was 543 nm, 633 nm and 633 nm, respectively. Emission was collected at 560–600 nm (SYTO-82), 650–700 nm (LTDR) and 650–700 nm (MTDR).

ICP-MS. HeLa cells were seeded in 10 cm tissue culture dishes and grown for 24 h. Then the cells were treated with complex **1–4** (2 μ M) for 12 h. The cells were then trypsinized and collected and washed with PBS twice. The cells were then counted. For whole cell platinum measurement, the HeLa cells were digested with HNO₃ (65%, 300 μ L) at room temperature for 24 h. The solution was then diluted to a final volume of 10 mL with Milli-Q water. For cytoplasm and nucleus platinum measurements, the cells cytoplasm and nucleus were extracted using a nucleus and cytoplasm extraction kit (Sangon, Shanghai, China). The samples were digested with 60% HNO₃ at room temperature for 24 h and then diluted to a final volume of 10 mL with Milli-Q water. The concentration of platinum was measured using the XSERIES 2 ICP-MS.

Cellular ROS production analysis. HeLa cells were seeded into 6-well plates (Corning) and incubated with **1–4** at the indicated concentrations for 12 h. The cells were further incubated with 10 μ M DCFH-DA in serum-free DMEM for 15 min at 37 °C. Then photoradiation (425 nm, 40 mW cm⁻², 15 min) was performed. After the treatment, the cells were collected and washed twice with serum-free DMEM. The fluorescence intensity of DCF in the cells was measured immediately by flow cytometry (FACSCalibur™, Becton Dickinson, Franklin Lakes, NJ, USA). Green mean fluorescence intensities were analyzed using FlowJo 7.6 software (Tree Star,

OR, USA).

PDT Activity. The cytotoxicity in the dark and phototoxicity of the tested compounds toward HeLa, HepG2, A549, A549cisR and LO2 cell lines was determined by MTT assay.

For cytotoxicity in the dark, cells were seeded in 96-well plates (Corning) and grown overnight. Then the cells were incubated with series concentration of the tested compounds for 44 h, 20 μ L MTT solution (5 mg/mL in PBS) was added to each well. The plates were incubated for another 4 h. Finally, the medium was carefully removed and the formazan product was dissolved in DMSO (150 μ L per well). The cell viability was evaluated by measurement of the absorbance at 490 nm (Infinite M200 Pro, Tecan, Männedorf, Switzerland). Each experiment was repeated at least three times to get the mean values.

For phototoxicity, the cells were incubated with the tested compounds for 12 h and then irradiated with a 425 nm LED light (40 mW cm^{-2}) for 15 min (36 J cm^{-2}). After another 32 h of incubation, MTT was added. The cytotoxicity was determined as described above. Vehicle-treated cells exposed to the light dose used did not show statistical viability difference to those in the dark.

Western blot analysis. HeLa cells were seeded into 60 mm tissue culture dishes (Corning) and cultured for 24 h, and then treated with complex **2** at the indicated concentrations for 24 h. Photoirradiation (425 nm, 40 mW cm^{-2} , 15 min) was performed after the cells were treated with **2** for 12 h. Cell lysates were prepared in radio immunoprecipitation assay (RIPA) buffer supplemented with inhibitors of proteases (Roche Diagnostics GmbH, Germany) and inhibitor of phosphatases sodium orthovanadate (Sigma Aldrich). Protein concentrations were quantified by a BCA protein assay reagent kit (Novagen Inc, USA). Equal amounts of protein were loaded and separated on SDS-polyacrylamide gel electrophoresis and then transferred onto polyvinylidene difluoride membranes (Millipore, USA). The membranes were blocked with 5% non-fat dry milk in TBST (20 mM Tris/HCl (pH 7.2)/150 mM NaCl/0.05% Tween-20) at room temperature for 2 h, and subsequently incubated with

primary antibodies specific to β -actin (Cell Signaling Technology, USA) and γ H2AX (Cell Signaling Technology, USA), H2AX (Cell Signaling Technology, USA) in TBST containing 5% nonfat milk at 4 °C overnight. After washing with TBST for three times the membranes were incubated with HRP-conjugated secondary antibody for 1 h at room temperature. The signals were detected using the enhanced chemiluminescence (ECL) kit (Amersham Inc, USA). Images were captured on FluorChem M (ProteinSimple, Santa Clara, CA).

Cell Cycle Analysis. HeLa cells were cultured in 6-well plates (Corning) and incubated with complex **2** at the indicated concentrations for 24 h. Photoirradiation (425 nm, 40 mW cm⁻², 15 min) was performed after the cells were treated with **2** for 12 h. The cells were collected and fixed in 2 mL 75% ethanol at 4 °C overnight. Cells were centrifuged and washed twice with cold PBS, and then resuspended in 500 μ L PBS containing 50 μ g/mL PI and 100 μ g/mL DNase-free RNase (Takara, Japan). Data were collected by a flow cytometer (FACSCalibur™, Becton Dickinson, Franklin Lakes, NJ, USA) and analyzed by ModFit LT 2.0 software (Variety Software House, Inc., Topsham, ME, USA).

Annexin V/Propidium Iodide Double Staining Assay. HeLa cells were cultured in 6-well plates (Corning) for 24 h and then treated with complex **2** at the indicated concentrations for 24 h. Photoirradiation (425 nm, 40 mW cm⁻², 15 min) was performed after the cells were treated with **2** for 12 h. The cells were collected and stained using an annexin V-FITC/propidium iodide apoptosis detection kit (Sigma Aldrich) according to the manufacturer's instructions. Data were collected by a flow cytometer (FACSCalibur™, Becton Dickinson, Franklin Lakes, NJ, USA) and analyzed with FlowJo 7.6 software (Tree Star, OR, USA).

In vivo PDT antitumor efficacy. Specific pathogen-free (SPF) female BALB/c nude mice, 4–5 weeks of age, were purchased and bred in the Experimental Animal Center of Sun Yat-Sen University. All animal operations were in accord with guidelines approved by the Sun Yat-Sen University Animal Care and Use Committee. HeLa xenograft-tumor model was established by subcutaneous injection of HeLa cells (1×10^6) into the right back flank of each nude mouse. When the tumor volume

reached approximately 150 mm³, the nude mice were randomly divided into five groups (5 mice per group) before drug treatments. Mice injected with physiological saline were the control group. Complex **2** was dissolved in physiological saline containing 1% DMSO. Mice were intratumorally injected with complex **2** at a dosage of 10 mg/kg body weight. After 2 h of the injection, the tumor region of the mice was irradiated with a 430 nm laser at 360 mW cm⁻² for 10 min. These treatments were administered with two repeated doses for 13 days. As for the positive control group, mice were also intratumorally injected with cisplatin (Sigma) at a dosage of 10 mg/kg body weight without light irradiation. Tumor sizes were measured once every 2 days using a digital caliper. Tumor volumes were calculated by the following formula: tumor volume = $ab^2 \times 0.5$, where a and b were the longest and the shortest diameters of the tumor. In the final of the experiment, the tumor tissues and major organs were harvested to make paraffin section for further H&E staining.

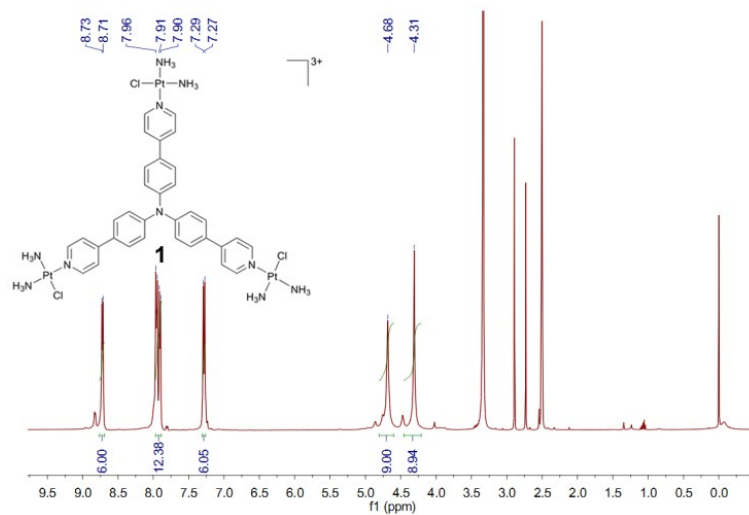


Figure S1. ¹H-NMR spectrum of **1** (400 MHz, *d*₆-DMSO).

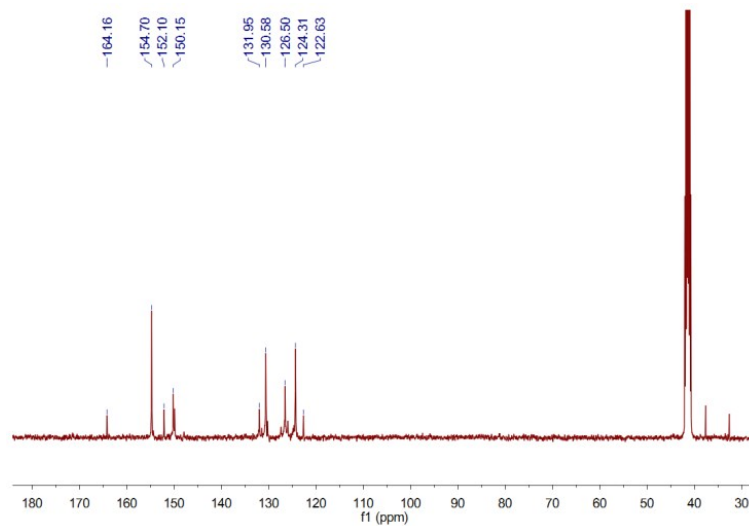


Figure S2. ¹³C-NMR spectrum of **1** (101 MHz, *d*₆-DMSO).

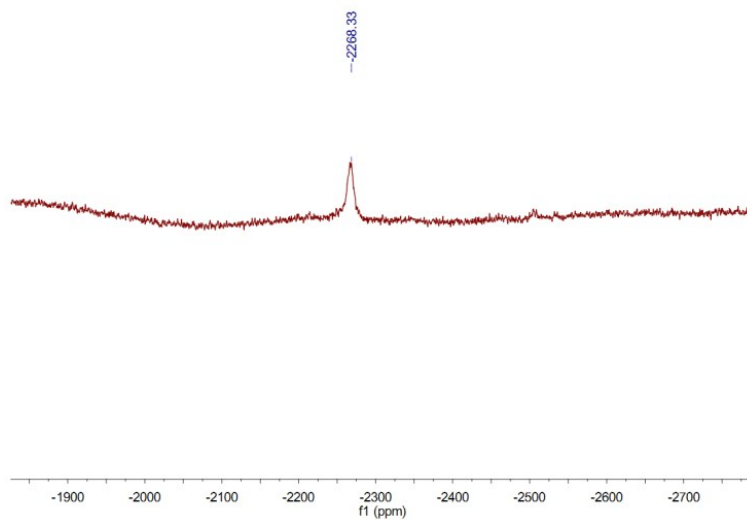


Figure S3. ^{195}Pt -NMR spectrum of **1** (86 MHz, d_6 -DMSO).

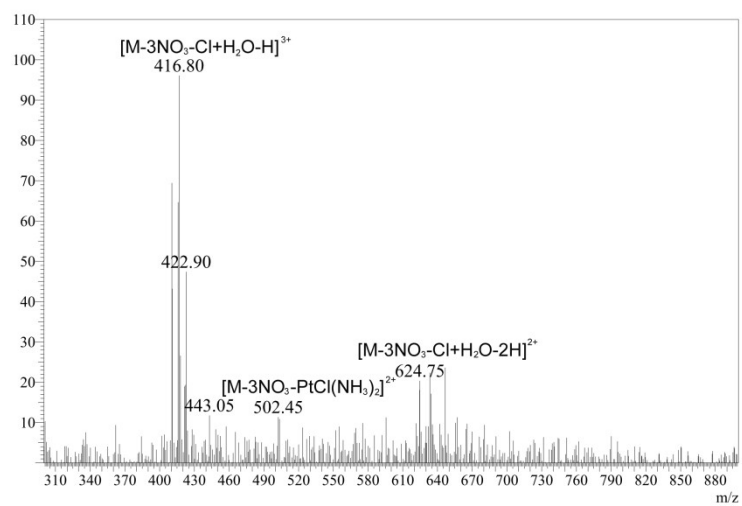


Figure S4. ESI-MS of complex **1** in water solution.

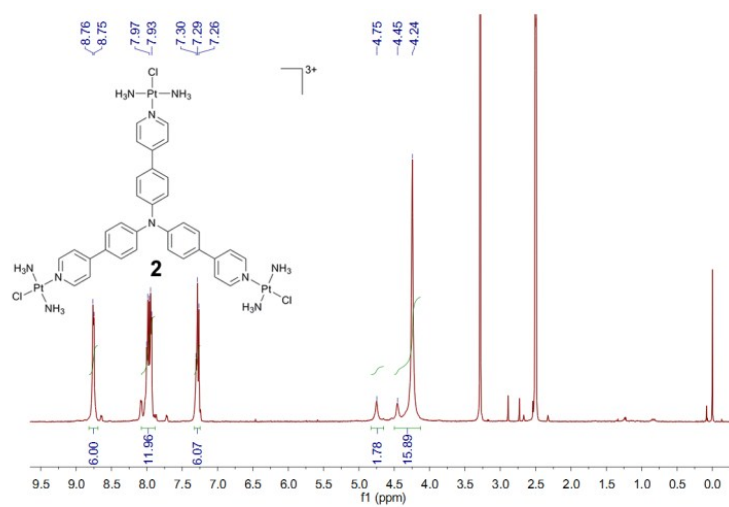


Figure S5. ¹H-NMR spectrum of **2** (400 MHz, *d*₆-DMSO).

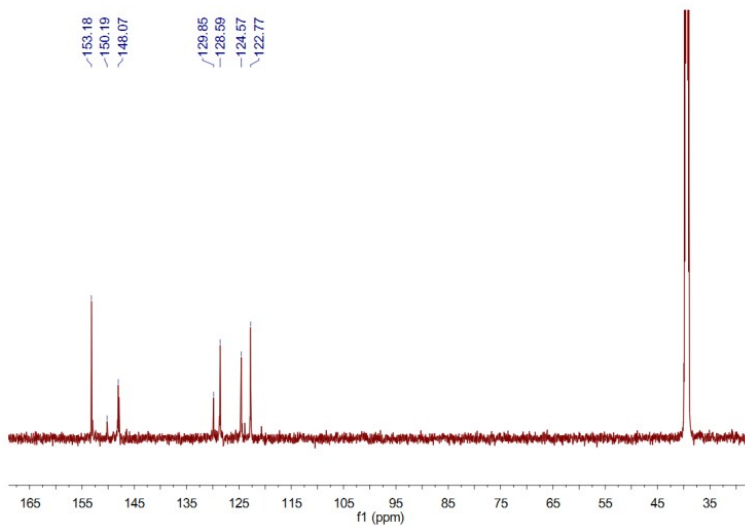


Figure S6. ¹³C-NMR spectrum of **2** (151 MHz, *d*₆-DMSO).

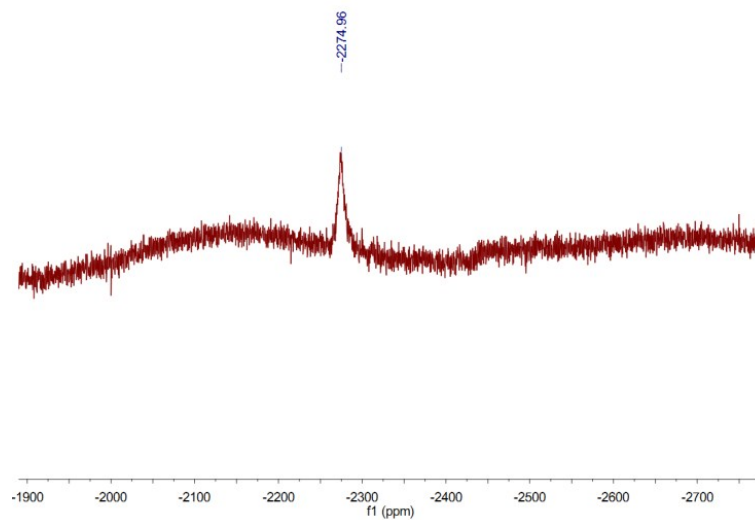


Figure S7. ^{195}Pt -NMR spectrum of **2** (86 MHz, d_6 -DMSO).

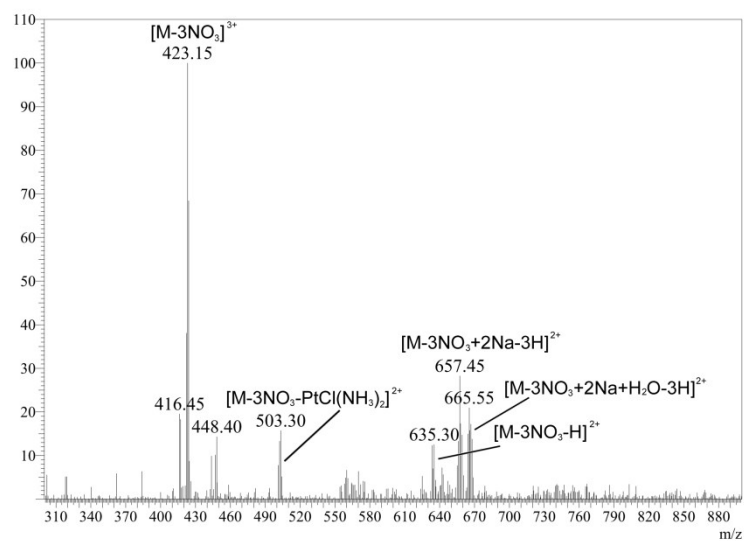


Figure S8. ESI-MS of complex **2** in water solution.

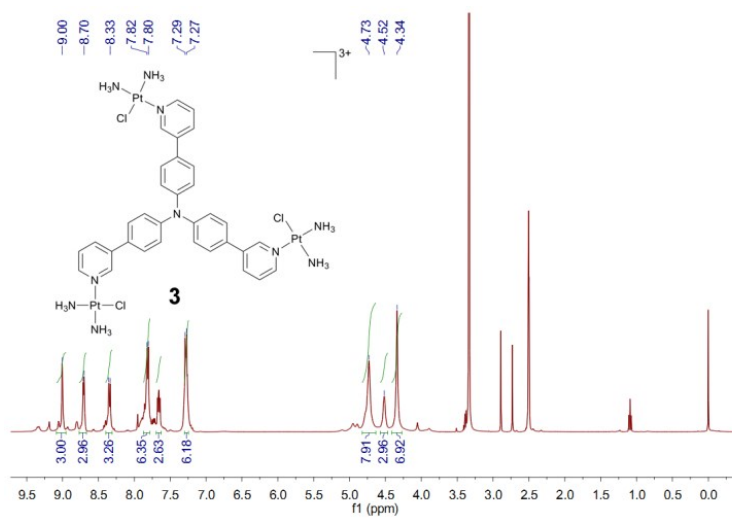


Figure S9. ¹H-NMR spectrum of **3** (400 MHz, *d*₆-DMSO).

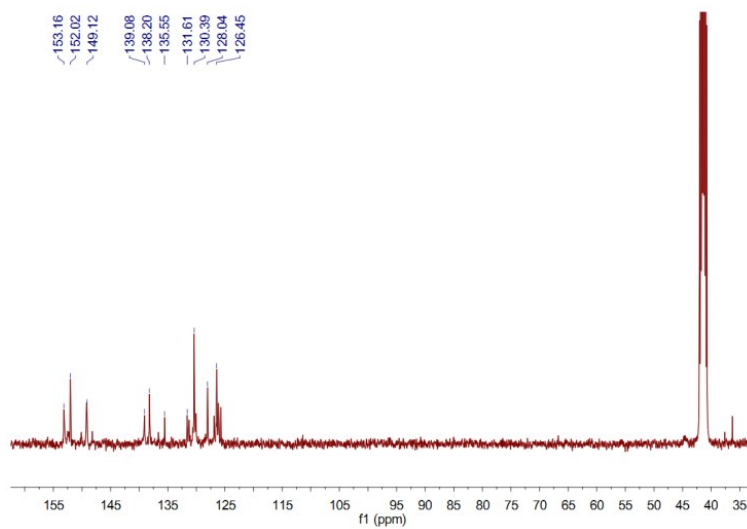


Figure S10. ¹³C-NMR spectrum of **3** (101 MHz, *d*₆-DMSO).

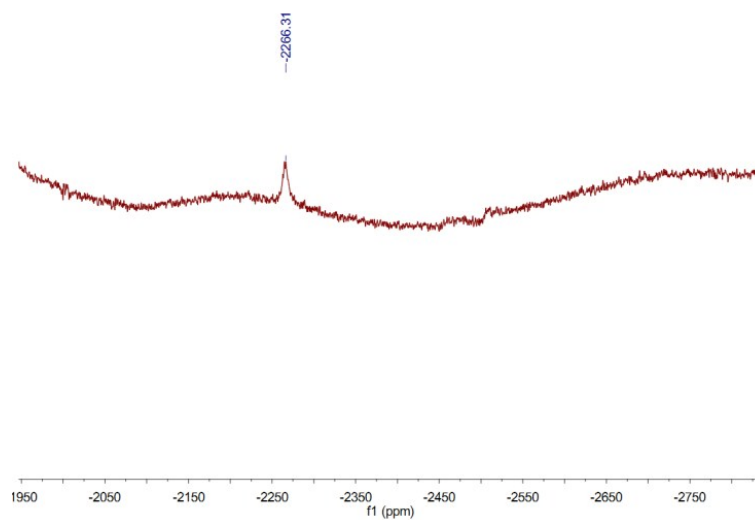


Figure S11. ^{195}Pt -NMR spectrum of **3** (86 MHz, d_6 -DMSO).

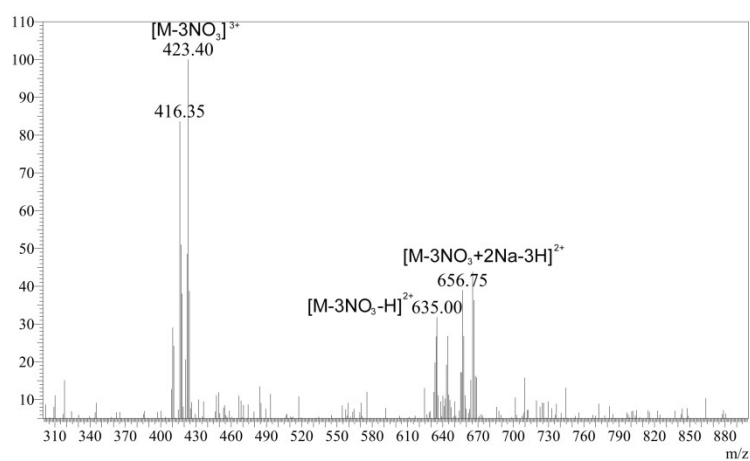


Figure S12. ESI-MS of complex **3** in water solution.

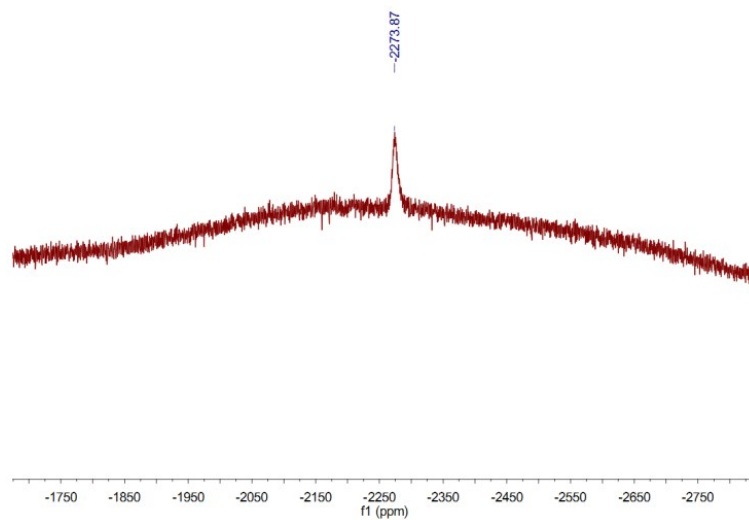


Figure S15. ^{195}Pt -NMR spectrum of **4** (86 MHz, d_6 -DMSO).

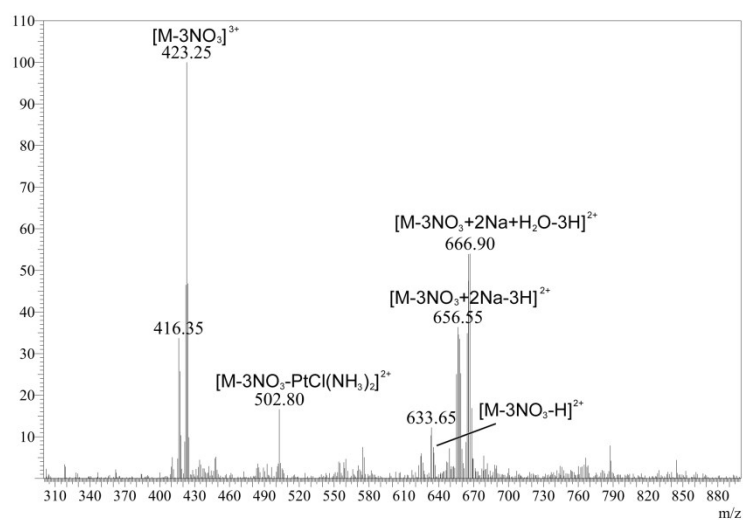


Figure S16. ESI-MS of complex **4** in water solution.

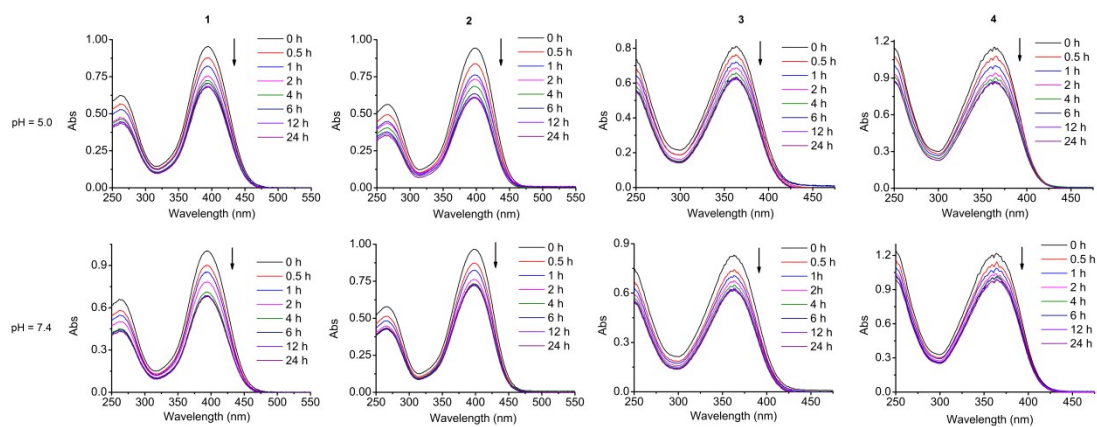


Figure S17. Time dependent UV-Vis spectra of complexes **1–4** in phosphate buffered saline (PBS) at pH = 5.0 and pH = 7.4.

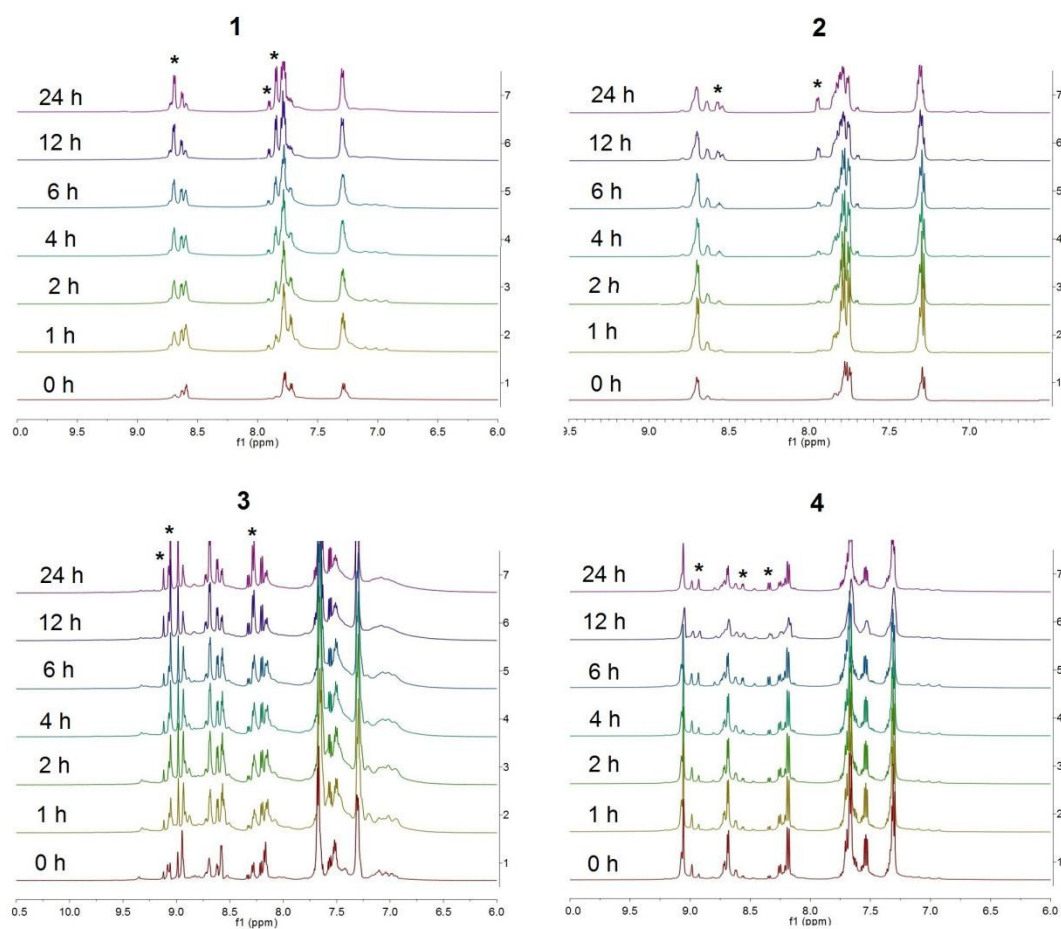


Figure S18. Time dependent ^1H -NMR spectra of **1–4** measured in d_6 -DMSO/ H_2O solution at 25 °C. “*” represented peaks with chemical shifts.

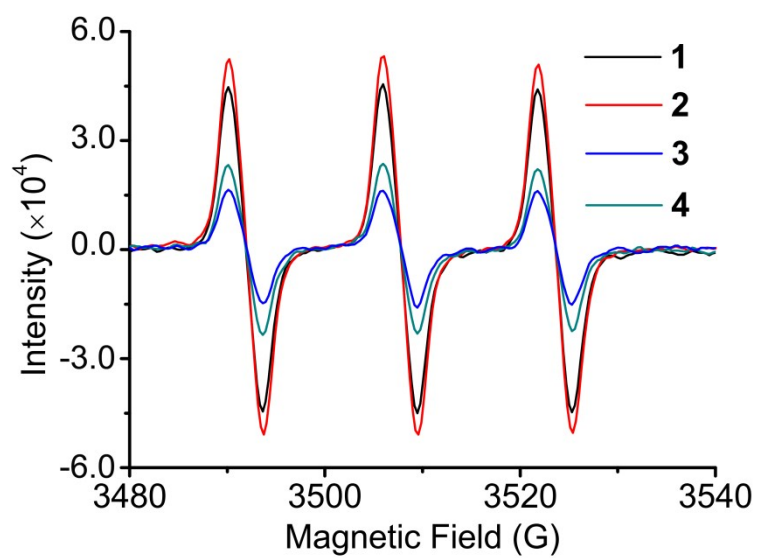


Figure S19. ESR signal of radicals induced by 1–4 and trapped by TEMP. Measurements were carried out in aerated 10 mM Tris-HCl, pH = 7.4 buffer under 425 nm light irradiation. TEMP is a spin trap of $^1\text{O}_2$.

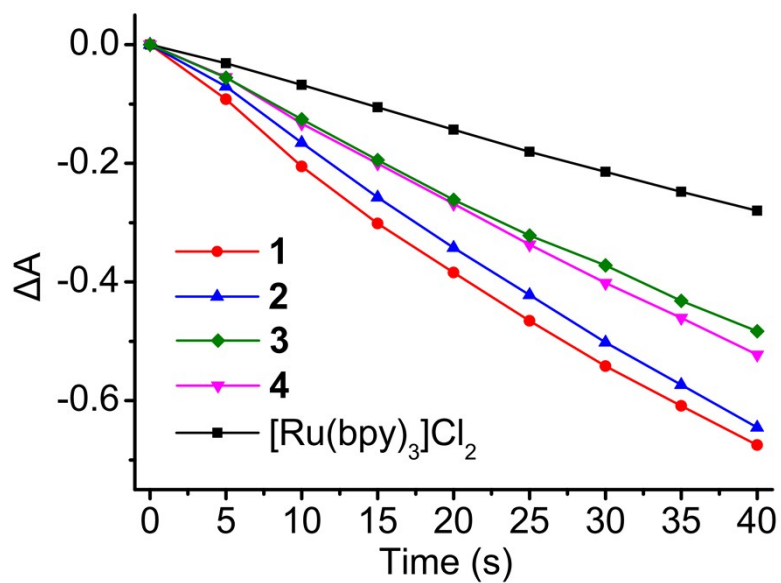


Figure S20. $^1\text{O}_2$ quantum yield of **1–4** measured by the decay of ABDA absorbance at 380 nm in 10 mM Tris-HCl, pH = 7.4 buffer under 365 nm irradiation. $[\text{Ru}(\text{bpy})_3]\text{Cl}_2$ served as standard.

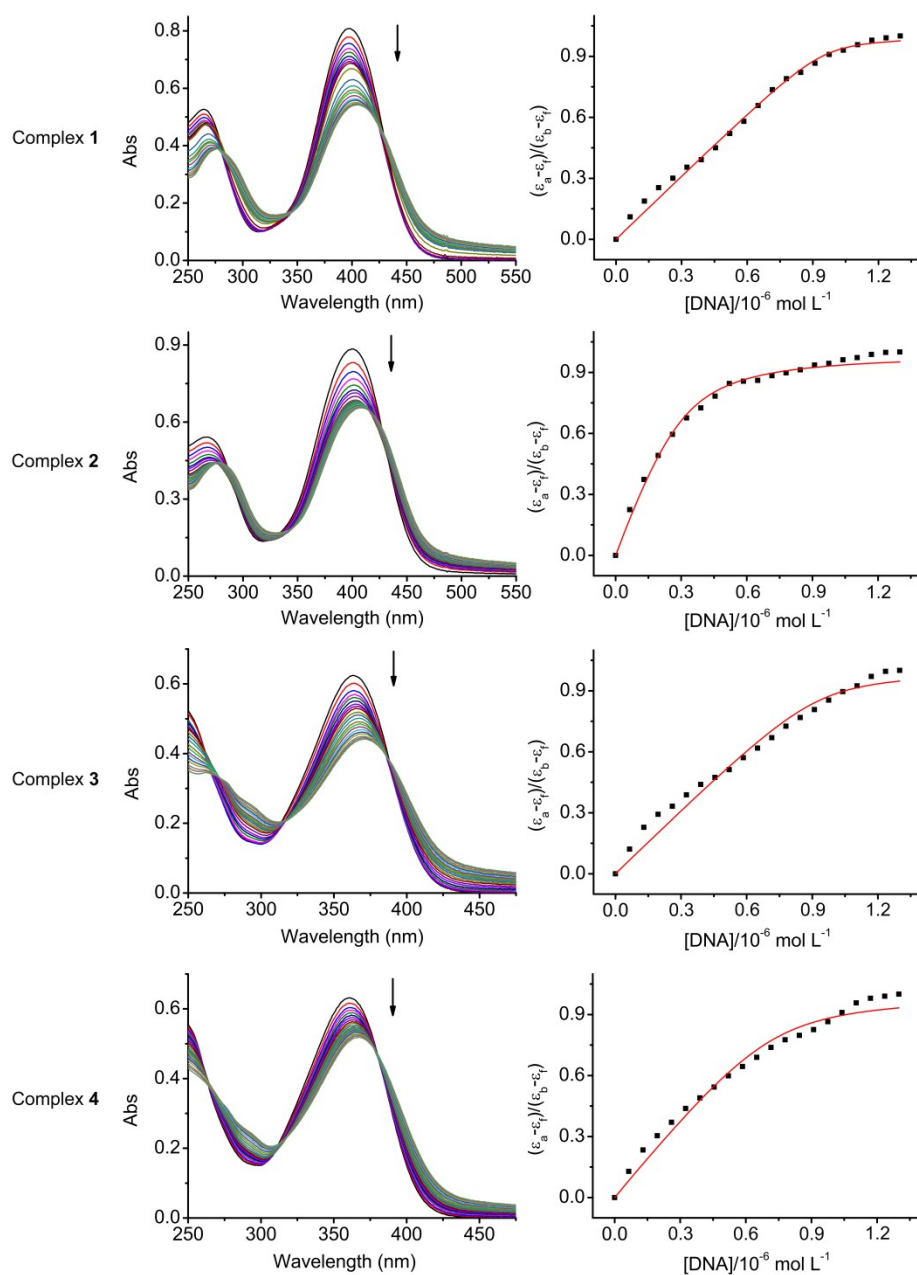


Figure S21. UV-Vis titration with single-stranded DNA (ssDNA) and calculation of the intrinsic binding constant K_b . Left: Change in the UV-Vis absorption spectra of **1–4** upon titration of ssDNA. Right: plot of $(\epsilon_a - \epsilon_f)/(\epsilon_b - \epsilon_f)$ vs. $[DNA]$. Buffer: 100 mM NaCl, 10 mM Tris-HCl, pH = 7.4.

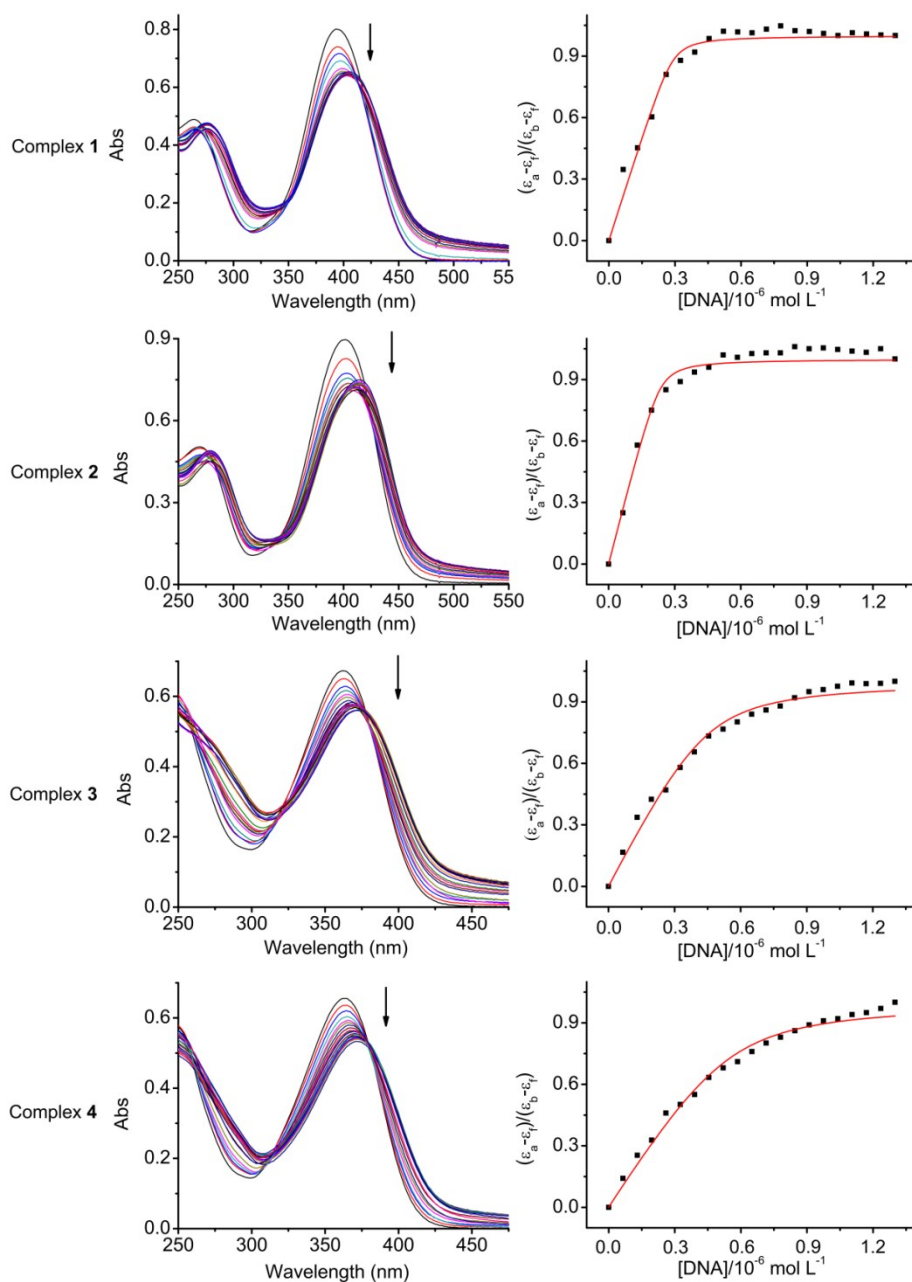


Figure S22. UV-Vis titration with duplex DNA (ds26) and calculation of the intrinsic binding constant K_b . Left: Change in the UV-Vis absorption spectra of **1–4** upon titration of ds26. Right: plot of $(\epsilon_a - \epsilon_f)/(\epsilon_b - \epsilon_f)$ vs. [DNA]. Buffer: 100 mM NaCl, 10 mM Tris-HCl, pH = 7.4.

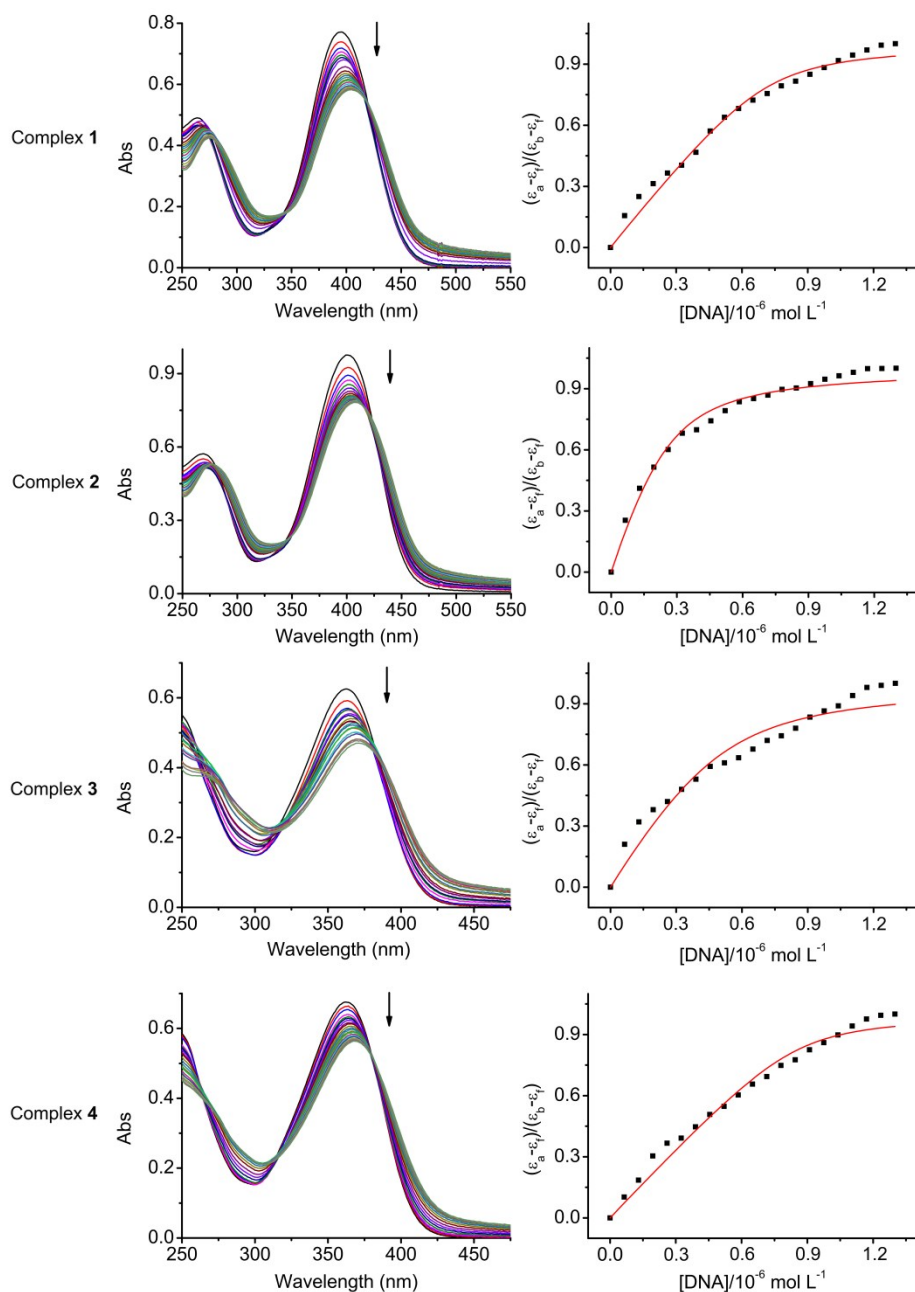


Figure S23. UV-Vis titration of G-quadruplex DNA (22AG) and calculation of the intrinsic binding constant K_b . Left: Change in the UV-Vis absorption spectra of 1–4 upon titration of 22AG. Right: plot of $(\epsilon_a - \epsilon_f)/(\epsilon_b - \epsilon_f)$ vs. [DNA]. Buffer: 100 mM KCl, 10 mM Tris-HCl, pH = 7.4.

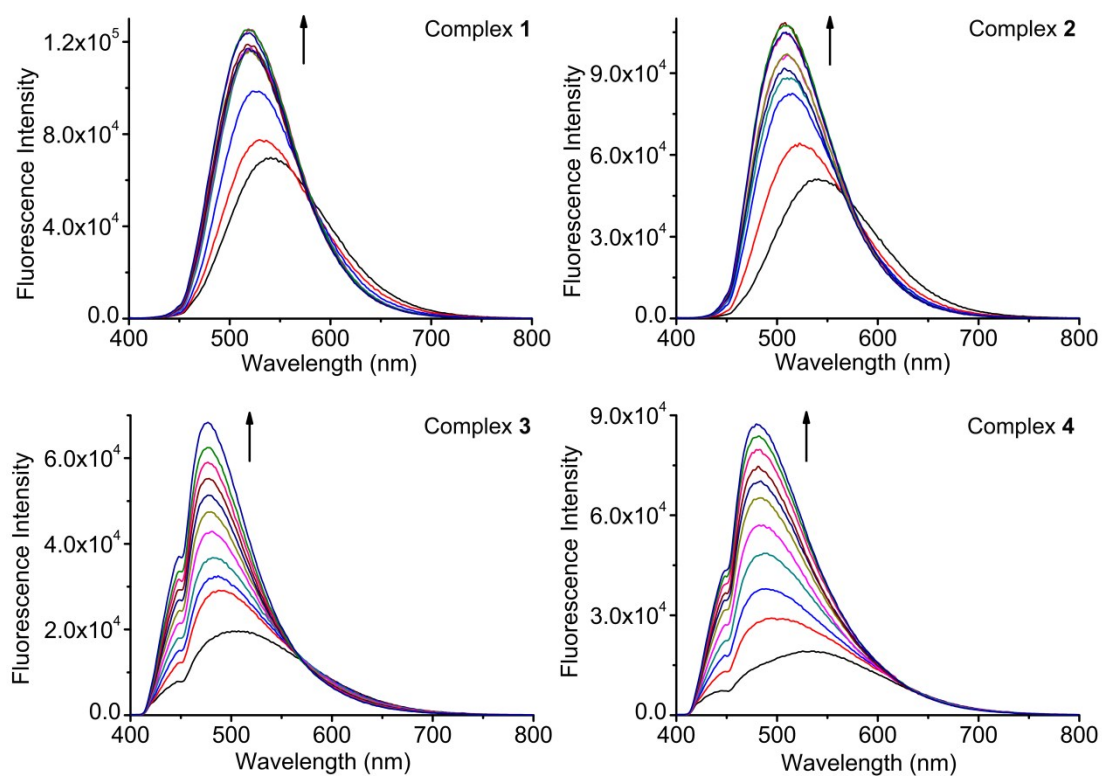


Figure S24. Fluorescence spectra change of **1–4** upon titration of single-stranded DNA (ssDNA). $\lambda_{\text{ex}} = 400 \text{ nm}$ for **1** and **2**. $\lambda_{\text{ex}} = 360 \text{ nm}$ for **3** and **4**. Buffer: 10 mM Tris-HCl, 100 mM NaCl, pH = 7.4.

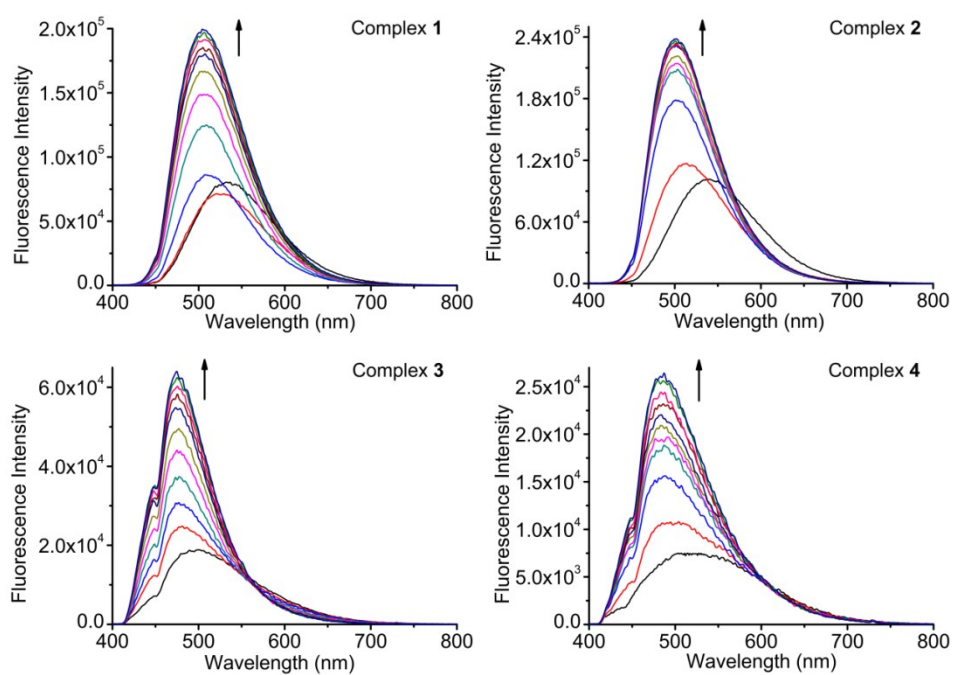


Figure S25. Fluorescence spectra change of **1–4** upon titration of duplex DNA (ds26). $\lambda_{\text{ex}} = 400 \text{ nm}$ for **1** and **2**. $\lambda_{\text{ex}} = 360 \text{ nm}$ for **3** and **4**. Buffer: 10 mM Tris-HCl, 100 mM NaCl, pH = 7.4.

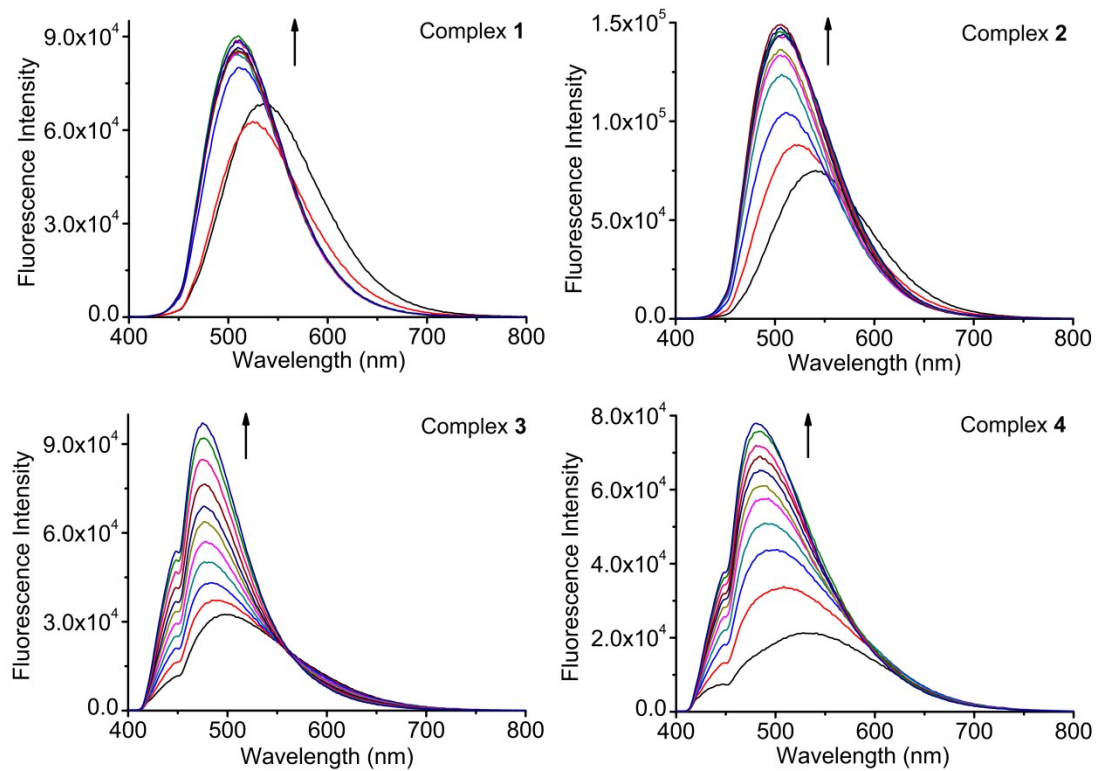


Figure S26. Fluorescence spectra change of **1–4** upon titration of G-quadruplex DNA (22AG). $\lambda_{\text{ex}} = 400$ nm for **1** and **2**. $\lambda_{\text{ex}} = 360$ nm for **3** and **4**. Buffer: 10 mM Tris-HCl, 100 mM KCl, pH = 7.4.

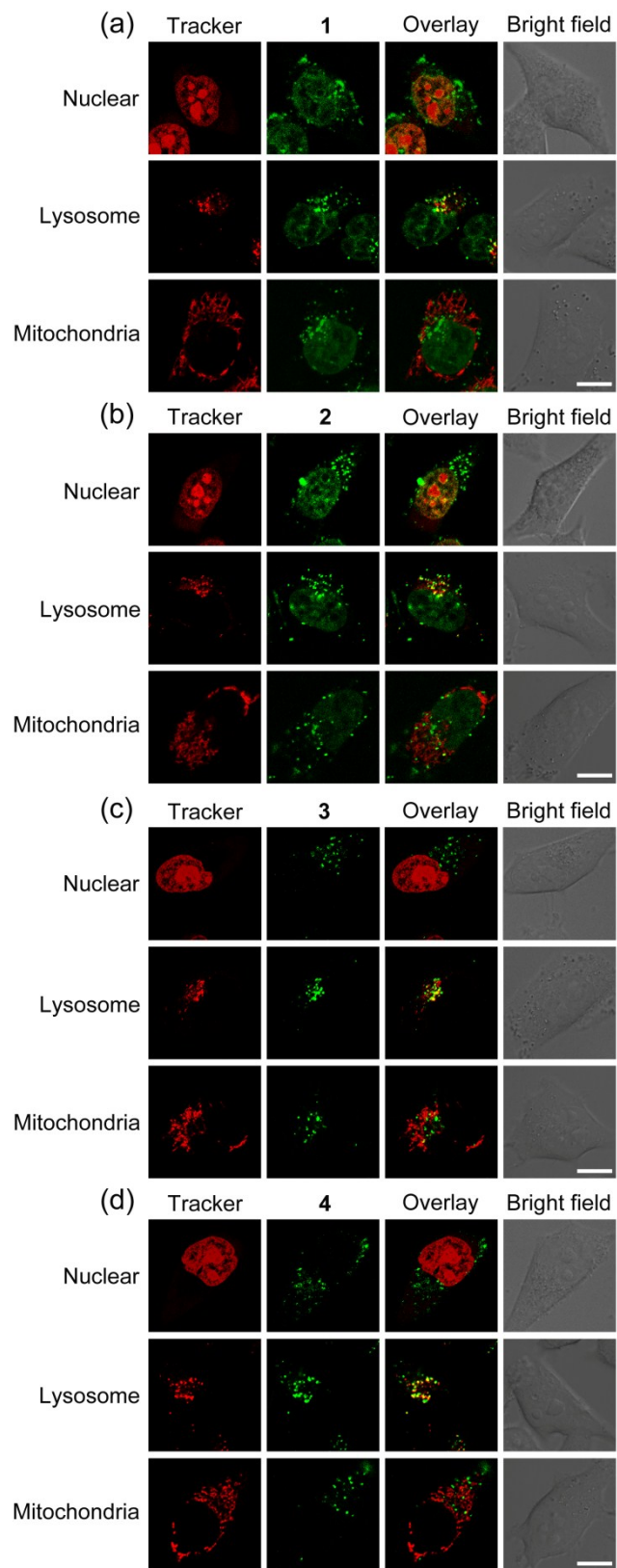


Figure S27. (a–d) Confocal microscopy images of HeLa cells coincubated with **1** (a), **2** (b), **3** (c), **4** (d) and commercial organelle trackers. HeLa cells were incubated with **1–4** (2 μM , 6 h) and then with nucleic acid stain SYTO-82 (1 μM , 0.5 h), lysosome tracker LTDR (150 nM, 0.5 h) or mitochondria tracker MTDR (150 nM, 0.5 h). For **1–4**, $\lambda_{\text{ex}} = 405 \text{ nm}$ and $\lambda_{\text{em}} = 480\text{--}580 \text{ nm}$. For SYTO-82, $\lambda_{\text{ex}} = 543 \text{ nm}$ and $\lambda_{\text{em}} = 560\text{--}600 \text{ nm}$. For LTDR and MTDR, $\lambda_{\text{ex}} = 633 \text{ nm}$ and $\lambda_{\text{em}} = 650\text{--}700 \text{ nm}$. Cells shown were representative images from replicate experiments ($n = 5$). Scale bar: 10 μm .

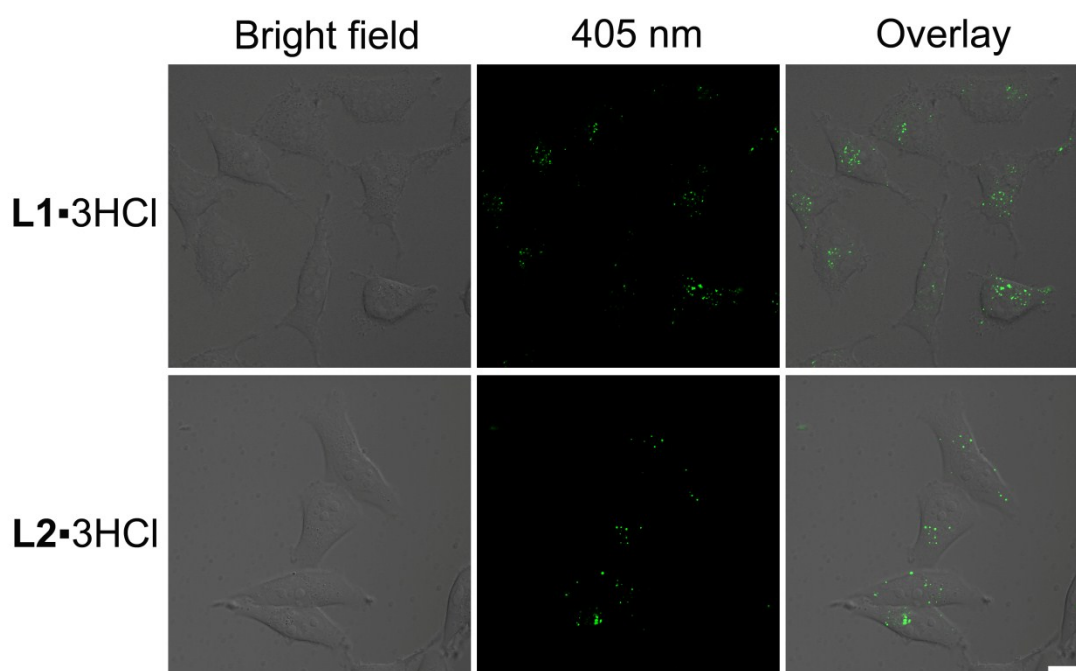


Figure S28. Confocal microscopy images of HeLa cells incubated with **L1•3HCl** and **L2•3HCl** (10 μM) for 12 h. $\lambda_{\text{ex}} = 405 \text{ nm}$ and light was collected at 460–560 nm. Cells shown were representative images from replicate experiments ($n = 5$). Scale bar: 10 μm .

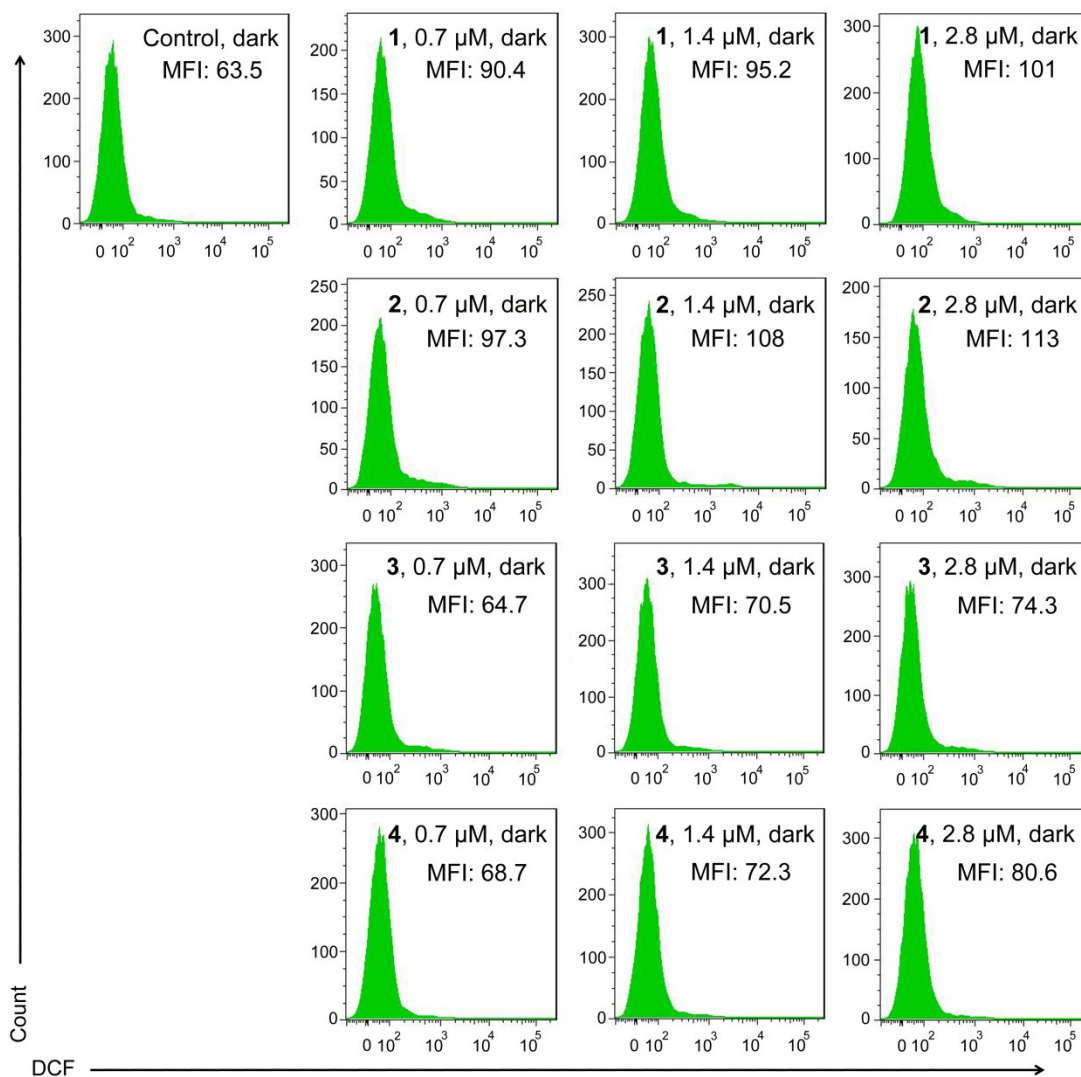


Figure S29. Effects of **1–4** on cellular ROS production in dark condition. DCFH-DA was used as a ROS probe. HeLa cells were incubated with **1–4** at 37 °C for 12 h, after which they were labeled with DCFH-DA and analyzed by flow cytometry. MFI: mean fluorescence intensity.

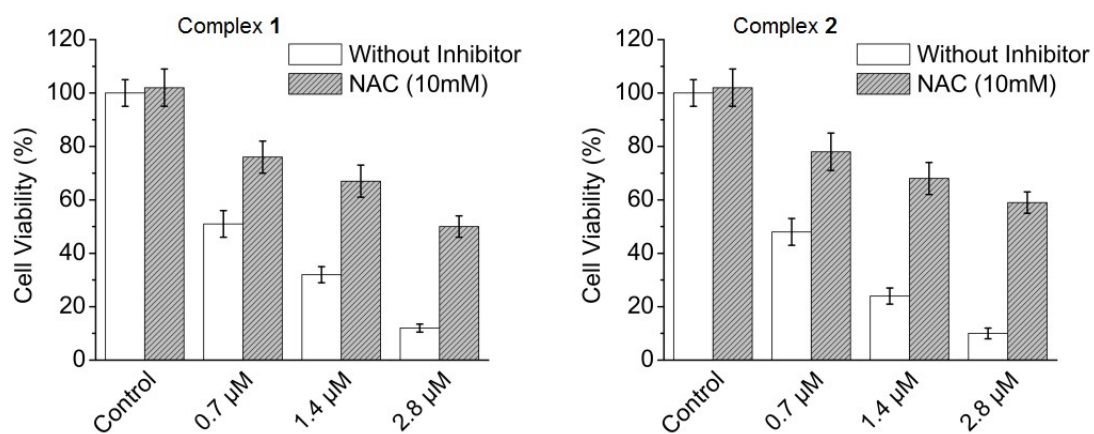


Figure S30. Effects of NAC on the viability of HeLa cells upon **1** and **2**- mediated PDT treatments. Data are presented as the mean \pm SD of three independent experiments.

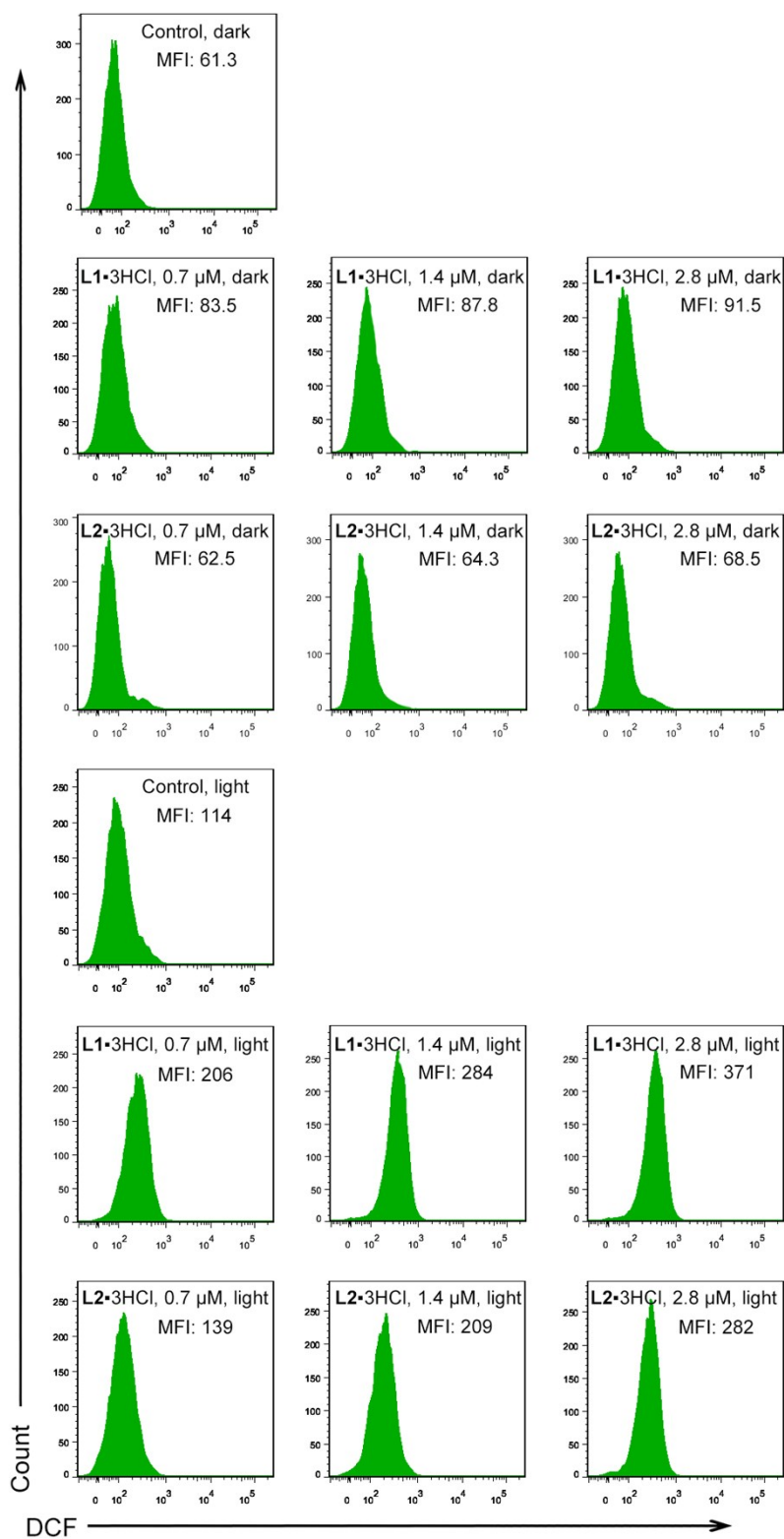


Figure S31. Effects of the bridging ligand L1 and L2 on cellular ROS production in the absence or presence of light at the indicated concentrations. DCFH-DA was used

as a ROS probe. Light: 425 nm, 40 mW cm⁻², 15 min. MFI: mean fluorescence intensity.

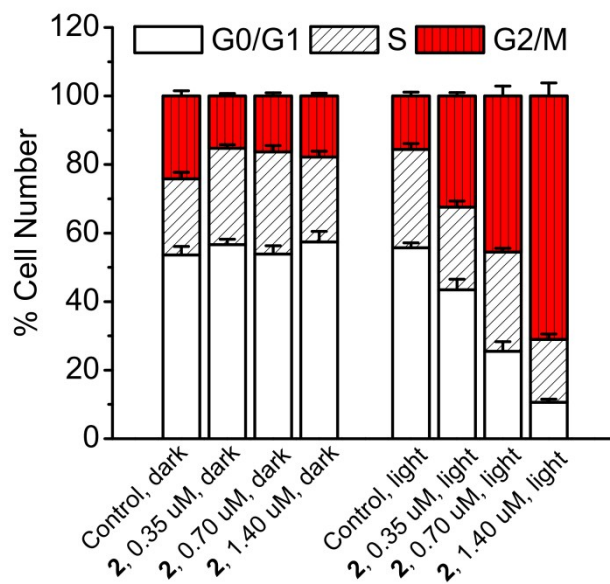


Figure S32. Quantitative cell-cycle distribution data for HeLa cells after treatment with **2** analyzed by flow cytometry. Dark: Cells were incubated with **2** for 24 h. Light: Cells were incubated with **2** for 12 h and then irradiated at 425 nm (40 mW cm⁻², 15 min) before incubated for another 12 h.

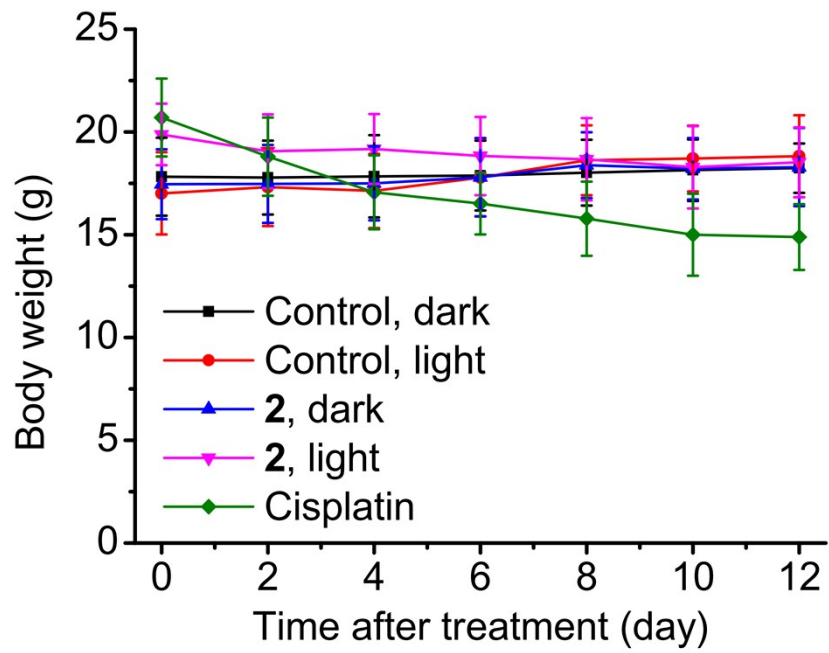


Figure S33. Body weight change of tumor-bearing mice with different treatments indicated (n = 5).

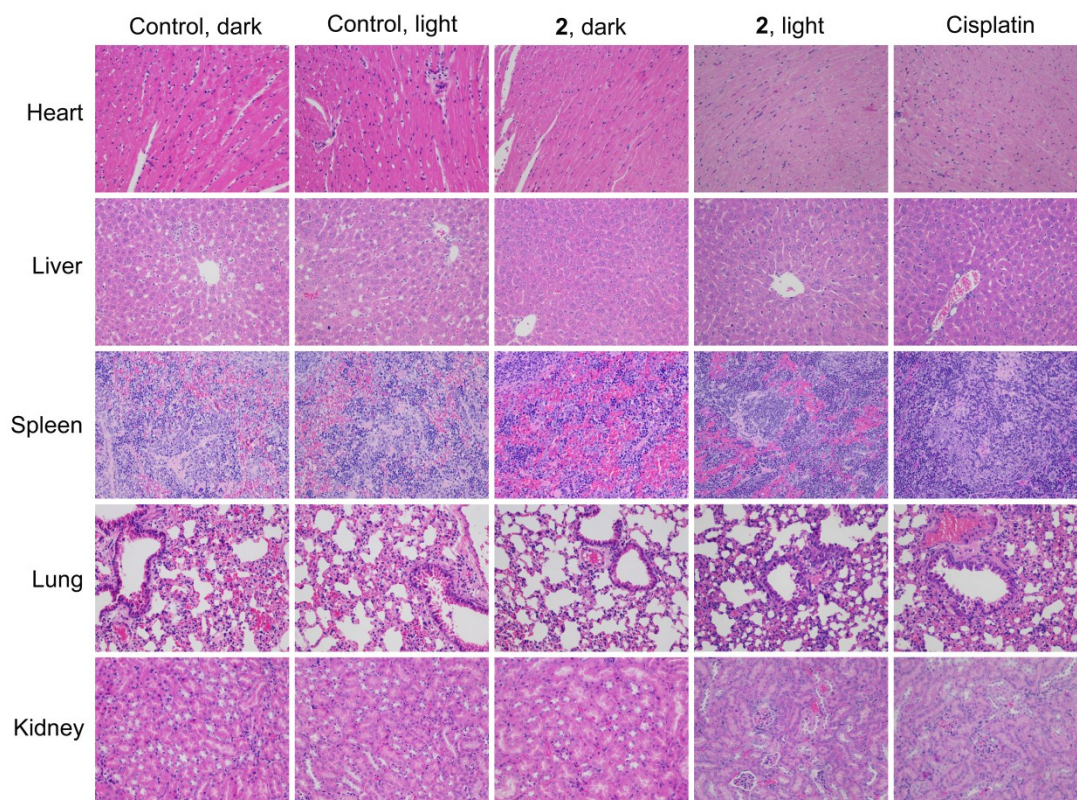


Figure S34 . H&E staining of the major organs of tumor-bearing mice after different treatments indicated.

Table S1. Summary of DNA binding constants of **1–4** measured by UV-Vis titration experiments.

Complex	K_b / M^{-1}		
	ssDNA	ds26	22AG
1	8.1×10^6	4.5×10^6	1.3×10^6
2	4.5×10^5	2.9×10^6	2.7×10^5
3	3.2×10^6	8.4×10^5	3.8×10^5
4	1.2×10^6	7.4×10^5	2.0×10^6

References

1. K. Nakamaru, *Bull. Chem. Soc. Jpn.* 1982, **55**, 2697–2705.
2. B. Hu, X. Chen, Y. Wang, P. Lu and Y. Wang, *Chem. Asian J.* 2013, **8**, 1144–1151.
3. H. Huang, B. Yu, P. Zhang, J. Huang, Y. Chen, G. Gasser, L. Ji, H. Chao, *Angew. Chem. Int. Ed.* 2015, **54**, 14049–14052.
4. J. S. Nam, M. G. Kang, J. Kang, S. Y. Park, S. J. C. Lee, H. T. Kim, J. K. Seo, O. H. Kwon, M. H. Lim, H. W. Rhee and T. H. Kwon, *J. Am. Chem. Soc.* 2016, **138**, 10968–10977.
5. B. A. Lindig, M. A. J. Rodgers, A. P. Schaap, *J. Am. Chem. Soc.* 1980, **102**, 5590–5593.
6. J. M. Wessels, C. S. Foote, W. E. Ford, M. A. J. Rodgers, *Photochem. Photobiol.* 1997, **65**, 96–102.
7. M. T. Carter, M. Rodriguez and A. J. Bard, *J. Am. Chem. Soc.* 1989, **111**, 8901–8911.

